

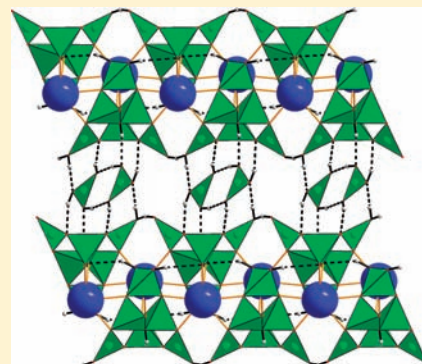
## Crystallization of New Samarium Polyborates

Zheng Ying Wu,<sup>†</sup> Paula Brandao, and Zhi Lin\*

Department of Chemistry, CICECO, University of Aveiro, 3810-193 Aveiro, Portugal

## Supporting Information

**ABSTRACT:** Rare earth borates are important due to their excellent properties, especially for optics. Here, we report the hydrothermal synthesis and structural determination by single-crystal X-ray diffraction of two new samarium polyborates with layered structures, being constituted by hexaborate chains. These hexaborate chains are connected by samarium polyhedra, forming dense sheets that further interact with each other by hydrogen bonding via isolated boric acid between these sheets. The third phase possesses a three-dimensional framework structure. The thermal stability of selective samples has been studied. The crystallization of samarium borate depends highly on the experimental conditions. Three samarium polyborates have been crystallized in very similar experimental conditions, clearly indicating that new lanthanide borate compounds with tailored structures may be prepared in the future by careful choice of physicochemical conditions.



## INTRODUCTION

Because of the extraordinary optical properties of many borates, the study of phase formation, structures, and properties of crystals in polyborate systems attracts many researchers.<sup>1–12</sup> For example,  $\text{BaB}_2\text{O}_4$  is a well-known common nonlinear optical material. Rare earth borates, a subgroup of this system, are of interest due to their luminescent,<sup>1–3</sup> nonlinear optical, and laser properties. Different synthesis strategies have been used in the preparation of rare earth polyborates, including high temperature/pressure, hydrothermal process, and boric acid flux method. Various structures have been identified. Different synthesis methods have their own advantages and disadvantages. The rare earth polyborates in the boron-rich region may not be stable at high temperature and also easily become glass. Hydrothermal synthesis and the boric acid flux method can be used to produce hydrous rare earth borates. By using molten boric acid, several new structures have been obtained, for example,  $\text{LnB}_6\text{O}_9(\text{OH})_3$  ( $\text{Ln} = \text{Sm}–\text{Lu}$ ),<sup>1</sup>  $\text{LnB}_8\text{O}_{11}(\text{OH})_5$  ( $\text{Ln} = \text{La}–\text{Nd}$ ),  $\text{LnB}_9\text{O}_{13}(\text{OH})_4 \cdot \text{H}_2\text{O}$  ( $\text{Ln} = \text{Pr}–\text{Eu}$ ),<sup>2</sup> and  $\text{Ln}_2\text{B}_6\text{O}_{10}(\text{OH})_4 \cdot \text{H}_2\text{O}$  ( $\text{Ln} = \text{Y}, \text{Pr}, \text{Nd}, \text{Sm}–\text{Gd}, \text{Dy}, \text{Ho}$ ).<sup>3</sup> In fact, in the synthesis using molten boric acid as flux, a small amount of water is generated in situ due to the reaction and condensation of boric acid, whereas in hydrothermal synthesis, more water is concerned in the precursor mixture. With the hydrothermal process,  $\text{NaNd}[\text{B}_6\text{O}_9(\text{OH})_4]_4$ ,<sup>4</sup>  $(\text{Nd}_{0.925}\text{Na}_{0.075})\text{-Nd}[\text{B}_9\text{O}_{15}(\text{OH})_2]\text{Cl}_{0.85} \cdot 2.65\text{H}_2\text{O}$ ,<sup>5</sup>  $\text{Ln}[\text{B}_4\text{O}_6(\text{OH})_2]\text{Cl}$  ( $\text{Ln} = \text{Pr}, \text{Nd}$ ),<sup>6</sup>  $\text{Y}[\text{B}_2\text{O}_3(\text{OH})]_3$ ,<sup>7</sup>  $\text{Ln}[\text{B}_5\text{O}_8(\text{OH})_2]$  ( $\text{Ln} = \text{La}, \text{Pr}, \text{Nd}$ ),<sup>8,9</sup>  $\text{LaB}_5\text{O}_8(\text{OH})_2 \cdot 1.5\text{H}_2\text{O}$ ,<sup>10</sup>  $\text{GdH}[\text{B}_2\text{O}_5]$ ,<sup>11</sup> and  $\text{LiNd}[\text{BO}_3(\text{OH})]^{12}$  have been synthesized. These works stimulate a search for new rare earth borates, especially under mild synthesis conditions. Indeed, novel polyborates are still discovered with time. The crystal structures of natural and synthetic borates have been reviewed by Belokoneva.<sup>13</sup> Here, we wish to report three samarium polyborates crystallized in very similar experimental conditions. Two of them possess new

layered structures. The new layered structures have been solved by single-crystal XRD data and compared to similar materials.

## EXPERIMENTAL SECTION

**Synthesis.** Samarium borates were synthesized hydrothermally with a small amount of water. A calculated amount of samarium chloride or nitrate was mixed with  $\text{H}_3\text{BO}_3$  and put into Teflon-lined autoclaves. Finally, water was added. The reactions were carried out at 220–240 °C for 2–21 days. The compositions and conditions used for obtaining different compounds are as follows.  $\text{H}_3\text{B}_7\text{SmO}_{16}$  (1):  $40\text{H}_3\text{BO}_3:\text{Sm}(\text{NO}_3)_3 \cdot 6\text{H}_2\text{O}:\text{H}_2\text{O}:\text{H}_2\text{O}$  at 230 °C for 10 days.  $\text{H}_{10}\text{B}_7\text{SmO}_{17}$  (2):  $40\text{H}_3\text{BO}_3:\text{SmCl}_3 \cdot 6\text{H}_2\text{O}:\text{H}_2\text{O}:\text{H}_2\text{O}$  at 230 °C for 10 days.  $\text{H}_6\text{B}_9\text{SmO}_{18}$  (3):  $40\text{H}_3\text{BO}_3:\text{SmCl}_3 \cdot 6\text{H}_2\text{O}:\text{H}_2\text{O}:\text{H}_2\text{O}$  at 220 °C for 10 days. The excess boric acid was removed by washing the products with hot distilled water, and the products were then dried at 60 °C overnight. These processes result in materials suitable for structure determination from single crystals (Figure S1 in the Supporting Information).

**Characterization.** The habit and crystal size of the samples were examined using scanning electron microscopy (SEM) on a Hitachi S-4100 microscope. The thermogravimetry (TG) curves were collected with a Shimadzu TG-50 analyzer. The samples were heated under air with a rate of 5 °C/min. The thermal stability and ion-exchange behavior of compound 2 were studied by X-ray powder diffraction (XRPD) on an X'Pert MPD Philips diffractometer (Cu  $K\alpha$  X-radiation).

**X-ray Crystallographic Studies.** The X-ray data were collected on a CCD Bruker APEX II at 150(2) K using graphite monochromatized Mo  $K\alpha$  radiation ( $\lambda = 0.71073$  Å). The crystals of compounds 1, 2, and 3 were positioned at 35 mm from the CCD, and the spots were measured using a counting time of 30 s for 1 and 2 and 10 s for 3. Data reduction, including a multiscan absorption correction, was carried out using the SAINT-NT from Bruker AXS. The structures were solved by direct methods and by subsequent difference Fourier syntheses and refined by full-matrix least-squares on

Received: November 22, 2011

Published: February 23, 2012

$F^2$  using the SHELX-97 suite.<sup>14</sup> The O–H and hydrogen atoms bonded to water molecules were located from final difference Fourier maps. Anisotropic thermal parameters were used for all non-hydrogen atoms, which were refined with isotropic thermal parameters equivalent to 1.2 times those of the atom to which they are attached. The crystallographic data of different phases are given in Table 1.

**Table 1. Crystal Data and Refinement Parameters of Samarium Borate Compounds 1, 2, and 3**

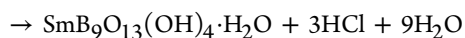
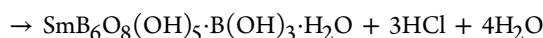
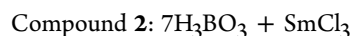
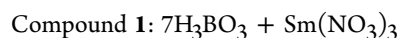
	1	2	3
empirical formula	H <sub>8</sub> B <sub>7</sub> SmO <sub>16</sub>	H <sub>10</sub> B <sub>7</sub> SmO <sub>17</sub>	H <sub>6</sub> B <sub>9</sub> SmO <sub>18</sub>
$M_w$	490.08	508.10	541.69
cryst syst	triclinic	monoclinic	monoclinic
space group	$P\bar{1}$	$C2/m$	$P2_1/n$
$a/[\text{Å}]$	6.8185(4)	8.7695(4)	7.6863(5)
$b/[\text{Å}]$	7.1522(5)	27.4712(9)	16.5408(9)
$c/[\text{Å}]$	12.6013(7)	6.8223(2)	9.8434(6)
$\alpha/[\text{deg}]$	94.746(4)	90	90
$\beta/[\text{deg}]$	99.049(4)	127.502(2)	90.073(3)
$\gamma/[\text{deg}]$	101.916(4)	90	90
$V[\text{Å}^3]$	589.57(6)	1303.88(8)	1251.46(13)
$Z$	2	4	4
$D_c [\text{Mg m}^{-3}]$	2.761	2.588	2.875
$\mu/[\text{mm}^{-1}]$	5.079	4.603	4.810
reflns collected	13 104	6870	38 924
unique reflns, $[R_{int}]$	4473 [0.0471]	3209 [0.0296]	4754 [0.0373]
final $R$ indices <sup>a</sup>			
$R_1, wR_2 [I > 2\sigma]$	0.0342, 0.0747 [3919]	0.0200, 0.0450 [2972]	0.0175, 0.0375 [4310]
$R_1, wR_2$ (all data)	0.0437, 0.0782	0.0237, 0.0486	0.0206, 0.0385

<sup>a</sup> $R_1 = \sum [|F_o| - |F_c|] / \sum |F_o|$ ;  $wR_2 = [\sum w(|F_o| - |F_c|)^2 / \sum w|F_o|^2]^{1/2}$ .

## RESULTS AND DISCUSSION

**Synthesis.** The synthesis of samarium borates is very sensitive to the experimental conditions. Slightly different starting reagents and temperatures can induce different structures. Although the synthesis of lanthanide borates has been studied systematically before, the formation of a new phase is still possible. In previous work,<sup>2</sup> samarium borates have been synthesized at 240 °C for 5 days with B/Sm ratios of 15 and 30 using Sm<sub>2</sub>O<sub>3</sub> as the Sm source, obtaining SmB<sub>6</sub>O<sub>9</sub>(OH)<sub>3</sub> and SmB<sub>9</sub>O<sub>13</sub>(OH)<sub>4</sub>·H<sub>2</sub>O (3), respectively. In our study, chloride and nitrate sources have been tested. Indeed, with the same B/Sm ratio (40), synthesis temperature (230 °C), and time (10 days), different structures have been formed in the reaction from chloride and nitrate sources. The nitrate source favors the formation of compound 1, whereas the chloride source induces the formation of compound 2. This difference may also be due to the slightly different water content in the synthesis or the postsynthesis washing process considering that the two structures are very similar. When chloride is used as the samarium source, the phase formation depends on the temperature and water content. At the H<sub>3</sub>BO<sub>3</sub>/SmCl<sub>3</sub>·6H<sub>2</sub>O ratio of 40, pure SmB<sub>9</sub>O<sub>13</sub>(OH)<sub>4</sub>·H<sub>2</sub>O (3) formed after the reaction at 230 °C for 10 days. If some water was added to the synthesis mixture (H<sub>2</sub>O/Sm = 26), a layered structure SmB<sub>6</sub>O<sub>8</sub>(OH)<sub>5</sub>·B(OH)<sub>3</sub>·H<sub>2</sub>O (2) was crystallized at this conditions with a trace amount of compound 3.

However, when the temperature was decreased to 220 °C for 10 days, the product was SmB<sub>9</sub>O<sub>13</sub>(OH)<sub>4</sub>·H<sub>2</sub>O (3). Furthermore, at the H<sub>3</sub>BO<sub>3</sub>/SmCl<sub>3</sub>·6H<sub>2</sub>O ratio of 40, pure SmB<sub>9</sub>O<sub>13</sub>(OH)<sub>4</sub>·H<sub>2</sub>O (3) formed at 240 °C for 10 days without any SmB<sub>6</sub>O<sub>9</sub>(OH)<sub>3</sub>, unlike the previous work<sup>2</sup> that a higher B/Sm ratio induced the formation of SmB<sub>6</sub>O<sub>9</sub>(OH)<sub>3</sub>. Of course, we could not rule out the influence of chlorine in the synthesis system. Meanwhile, the synthesis with the nitrate source did not give any SmB<sub>9</sub>O<sub>13</sub>(OH)<sub>4</sub>·H<sub>2</sub>O (3). The formation of different compounds can be represented by the following reactions:



The above formulas indicate that these reactions would produce hydrochloric acid or nitric acid. Indeed, the stainless autoclaves are easily corroded in these syntheses due to the high volatility of HCl or HNO<sub>3</sub> at high temperature, although they are Teflon-lined. On the other hand, this also indicates that the reaction condition here is strongly acidic, different to the previous one.<sup>2</sup> At similar experimental conditions, we did not get these layered structures for other rare earth elements.

**Structure of Compound 1 [SmB<sub>6</sub>O<sub>8</sub>(OH)<sub>5</sub>·B(OH)<sub>3</sub>].** Single-crystal X-ray analysis indicates that the asymmetric unit of compound 1 contains one crystallographically unique Sm<sup>3+</sup> ion, four BO<sub>4</sub> tetrahedral units, two BO<sub>3</sub> trigonal units, and one extra lattice boric acid molecule, B(OH)<sub>3</sub> (Figure 1a). The geometry about the eight-coordinate samarium metal center can be best described as a square antiprism (see Figure S2a in the Supporting Information), with Sm–O bond distances varying from 2.409(2) to 2.504(2) Å and O–Sm–O angles changing from 56.18(8) to 168.99(9)°; all O atoms are bridged by B centers. The BO<sub>4</sub> tetrahedral and BO<sub>3</sub> trigonal units form a chain along the *a* axis. The chain can be described using a fundamental building block (FBB),<sup>13</sup> containing 4T + 2Δ (B<sub>6</sub>O<sub>8</sub>(OH)<sub>5</sub>) units. The B–O bond distances vary from 1.343(5) to 1.396(5) Å for the BO<sub>3</sub> trigonal unit and 1.437(4) to 1.496(5) Å for the BO<sub>4</sub> tetrahedra. The O–B–O angles are distributed in the range of 115.9(3)–124.8(3)° for the B trigonal unit and 102.2(3)–114.7(3)° for B tetrahedra. Selected bond lengths and angles for compound 1 are listed in Table S1 in the Supporting Information. The compound charge neutrality is achieved by the presence of OH groups; these hydrogen atoms were located from final difference Fourier maps. Compound 1 is constructed by parallel packing, in the *ab* plane, of two-dimensional [SmB<sub>6</sub>O<sub>8</sub>(OH)<sub>5</sub>]<sub>∞</sub> layers (see Figure 1b,c), which are formed via edge- and corner-sharing between borate chains and samarium polyhedra. The borate chains wind around samarium polyhedra. The neutral boric acid molecules found between these layers interact with the oxygen atoms of layers through four O–H···O hydrogen bonds with O···O distances between 2.572(4) and 2.747(4) Å (Table 2), resulting in a 2D supramolecular structure, as illustrated in Figure 1b. The boric acid molecules also interact among themselves

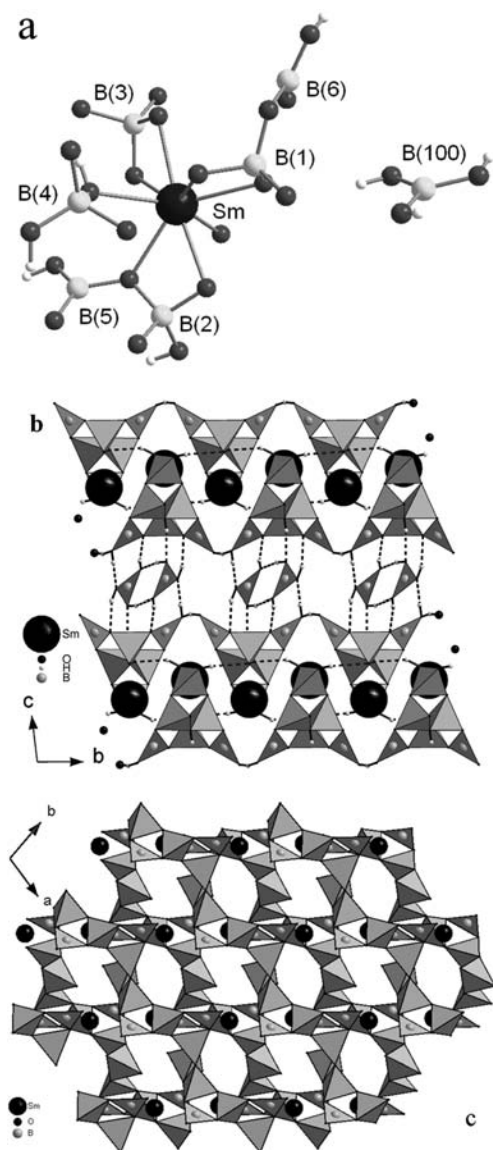


**Figure 1.** Structure of compound 1: (a) asymmetric unit; (b) crystal packing viewed along the  $a$  axis; dashed lines represent O–H...O hydrogen bond interactions; (c) a top view of the  $[\text{SmB}_6\text{O}_8(\text{OH})_5]_\infty$  layer. The triangles and tetrahedra represent three- and four-coordinated B.

through O–H...O hydrogen bonds, generating hexagonal rings along the  $a$  axis (Table 2).

**Structure of Compound 2**  $[\text{SmB}_6\text{O}_8(\text{OH})_5 \cdot \text{B}(\text{OH})_3 \cdot \text{H}_2\text{O}]$ . Compound 2 shows some structural similarities to compound 1 (Figure 2). It is also built up of parallel packing, in the  $ac$  plane, of two-dimensional  $[\text{SmB}_6\text{O}_8(\text{OH})_5]_\infty$  layers (Figure 2c), containing polyborate chain forming from  $4\text{T} + 2\Delta$  units along the  $c$  axis. Nevertheless, compound 2 crystallizes in the monoclinic system with  $C2/m$  symmetry. The asymmetric unit consists of one unique crystallographic  $\text{Sm}^{3+}$  ion with an occupancy factor of 0.5, three  $\text{BO}_4$  tetrahedra (two with an occupancy factor of 0.5), one  $\text{BO}_3$  trigonal, and one extra lattice boric acid molecule and one water molecule, both with an occupancy factor of 0.5 (see Figure 2a). The samarium center is surrounded by eight oxygens bridging with B centers exhibiting a square antiprismatic coordination (see Figure S2b in the Supporting Information). The Sm–O distances lie in the

**Table 2.** Hydrogen-Bonding Parameters of Samarium Borate Compounds

D–H...A	H...A/Å	D...A/Å	D–H...A/deg
compound 1			
O(7)–H(7)...O(11) $[-x, 1 - y, 1 - z]$	2.10(5)	2.891(4)	149(5)
O(10)–H(10)...O(1) $[1 - x, -y, 1 - z]$	2.30(6)	3.021(4)	168(4)
O(12)–H(12)...O(13) $[-x, -y, 1 - z]$	1.90(4)	2.731(4)	178(6)
O(9)–H(9)...O(101) $[x, y, z - 1]$	1.82(2)	2.572(4)	151(5)
O(13)–H(13)...O(102) $[1 - x, 1 - y, 1 - z]$	1.90(4)	2.731(4)	178(6)
O(102)–H(102)...O(2) $[1 - x, 1 - y, 2 - z]$	1.94(3)	2.747(4)	163(5)
O(103)–H(103)...O(6)	1.90(5)	2.683(4)	158(5)
O(101)–H(101)...O(103) $[-x, 1 - y, 2 - z]$	1.81(4)	2.626(4)	169(5)
compound 2			
O(2)–H(2)...O(100)	1.63(8)	2.445(3)	167(6)
O(2)–H(2)...O(100) $[1 - x, y, 2 - z]$	1.63(8)	2.445(3)	167(6)
O(3)–H(3)...O(6) $[1/2 - x, 1/2 - y, 2 - z]$	2.16(2)	2.908(2)	151(2)
O(7)–H(7)...O(101)	1.97(2)	2.765(2)	163(4)
O(102)–H(102)...O(1)	1.90(3)	2.706(2)	164(3)
compound 3			
O(2)–H(2)...O(14) $[-x, 1 - y, 2 - z]$	1.92(2)	2.723(2)	167(2)
O(6)–H(6)...O(2) $[1/2 - x, y - 1/2, 3/2 - z]$	1.89(2)	2.644(2)	164(2)
O(8)–H(8)...O(11) $[3/2 - x, y - 1/2, 3/2 - z]$	2.48(2)	3.185(2)	156(2)
O(100)–H(10A)...O(1) $[x - 1, y, z]$	2.35(3)	3.087(2)	149(2)
O(100)–H(10B)...O(3) $[x - 1, y, z]$	2.18(2)	2.986(2)	167(2)
O(17)–H(17)...O(100) $[x + 1/2, 1/2 - y, z + 1/2]$	1.97(2)	2.723(2)	164(2)

2.416(2)–2.488(4) Å range, and the O–Sm–O bond angles span from  $56.03(4)$  to  $169.72(4)^\circ$ . The B–O distances vary from 1.361(2) to 1.381(2) Å and from 1.448(2) to 1.489(9) Å, and the O–B–O bond angles are in the range of  $118.06(15)$ – $121.65(16)^\circ$  and  $103.98(7)$ – $115.41(19)^\circ$  for  $\text{BO}_3$  and  $\text{BO}_4$  units, respectively. Selected bond lengths and angles for compound 2 are listed in Table S2 in the Supporting Information. The neutral boric acid and the water molecules are found between layers, establishing O–H...O hydrogen bonds with O...O distances between 2.445(3) and 2.706(2) Å (Figure 2b and Table 2), forming a 2D supramolecular structure.

**Structure of Compound 3**  $[\text{SmB}_9\text{O}_{13}(\text{OH})_4 \cdot \text{H}_2\text{O}]$ . Single-crystal X-ray analysis indicates that compound 3 crystallizes in the monoclinic system with  $P2_1/n$  symmetry. The asymmetric unit of compound 3 contains one  $\text{SmO}_9$ , five  $\text{BO}_4$  and four  $\text{BO}_3$  units, and one extra lattice water molecule, as shown in Figure 3a. The extended linkage of this asymmetric building unit yields a three-dimensional network with intersecting channels along the  $[100]$  and  $[001]$  directions, where are allocated the water molecules. The charge neutrality of the  $[\text{SmB}_9\text{O}_{13}]^{+4}$  layer is achieved by the presence of four OH groups. The  $\text{Sm}^{3+}$  ion is coordinated to nine oxygen atoms, in which four are due to edge-sharing with two  $\text{BO}_4$  tetrahedra and five are due to edge-sharing with two  $\text{BO}_3$  triangles and corner-sharing with a  $\text{BO}_3$  triangle, with the overall coordination geometry of a tricapped trigonal prismatic (see Figure S2c in the Supporting Information). The Sm–O bond distances varying from 2.318(1) to 2.599(6) Å and O–Sm–O angles changing from  $54.34(4)$  to  $173.65(4)^\circ$ . The boron atoms assume two kinds of

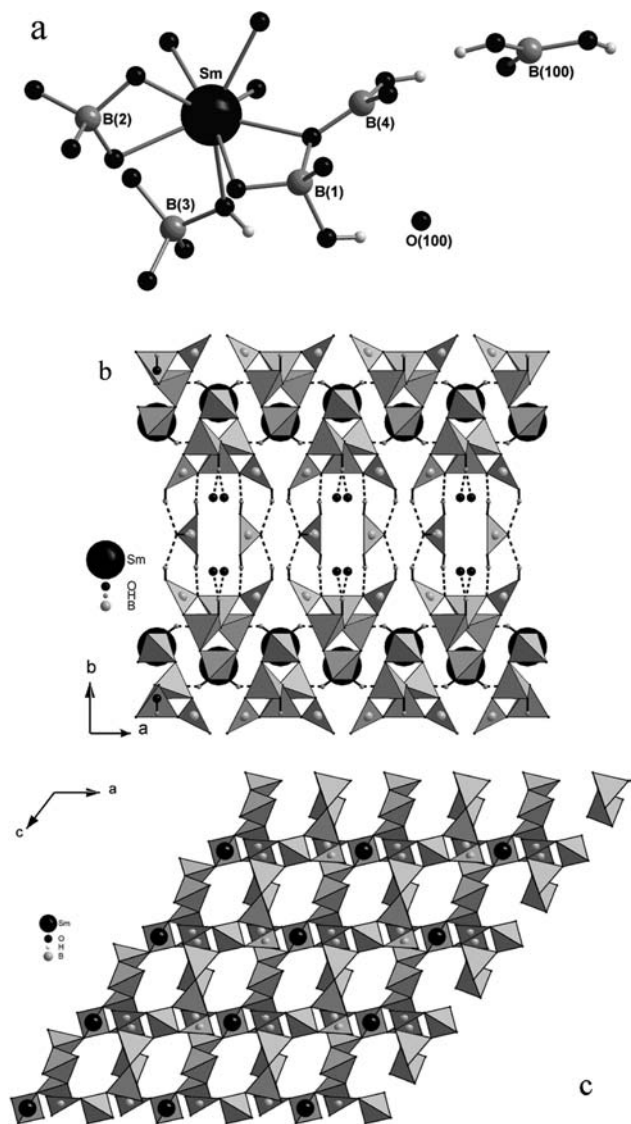


**Figure 2.** Structure of compound 2: (a) asymmetric unit; (b) crystal packing along the  $c$  axis; dashed lines represent O–H...O hydrogen bond interactions; (c) a top view of the  $[\text{SmB}_6\text{O}_8(\text{OH})_5]_\infty$  layer. The triangles and tetrahedra represent three- and four-coordinated B.

coordination models with B–O bond distances varying from 1.351(2) to 1.397(2) Å for the  $\text{BO}_3$  trigonal unit and 1.397(2) to 1.556(2) Å for the  $\text{BO}_4$  tetrahedral unit. The O–B–O angles are distributed in the range of  $113.13(15)$ – $124.76(15)^\circ$  for the trigonal ones and  $102.88(13)$ – $114.73(13)^\circ$  for the tetrahedral ones. Selected bond lengths and angles for compound 3 are listed in Table S3 in the Supporting Information. The borate units polymerized in two types of clusters (see Figure S3 in the Supporting Information):  $\text{B}_6\text{O}_{14}$  is made up from four  $\text{BO}_4$  tetrahedra and two  $\text{BO}_3$  triangles (cluster 1:  $4\text{T} + 2\Delta$ ), and a second  $\text{B}_6\text{O}_{11}$  cluster is built up from three  $\text{BO}_4$  tetrahedra and three  $\text{BO}_3$  triangles (cluster 2:  $3\text{T} + 3\Delta$ ). In cluster 1, four  $\text{BO}_4$  tetrahedra form a four-membered ring by corner-sharing one oxygen atom. Cluster 1 does not connect to the same type. In cluster 2, three  $\text{BO}_4$  tetrahedra share one oxygen atom. Cluster 2 connects to each other by  $\text{BO}_3$ . Cluster 1 and 2 connect to each other by two  $\text{BO}_4$  tetrahedra from different clusters via corner-sharing oxygen. The combination of these two clusters forms a 3D borate framework, and the  $\text{SmO}_9$  incorporate into

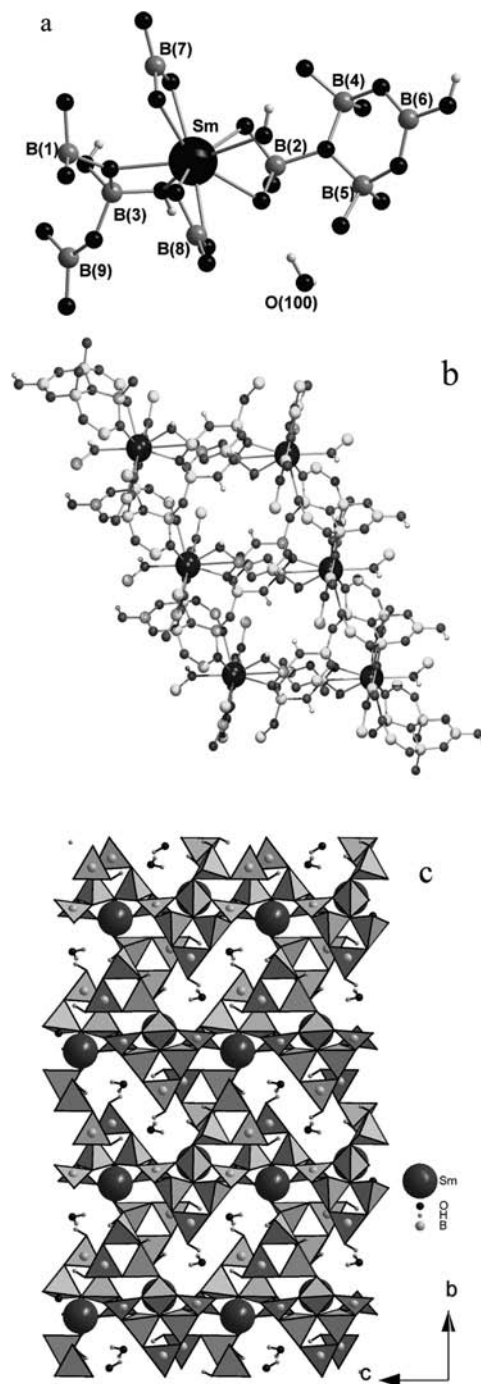


**Figure 3.** Structure of compound 3: (a) asymmetric unit; (b) a one-dimensional chain structure linkage of  $\text{B}_6\text{O}_{14}$  and  $\text{B}_6\text{O}_{11}$  clusters and  $\text{SmO}_9$  groups along the  $c$  axis; (c) 3D network along the  $a$  axis. The triangles and tetrahedra represent three- and four-coordinated B.

the 3D structure through their edges or corners (Figure 3b,c). The hydrogen bonds in compound 3 are listed in Table 2. In the literature,<sup>2</sup> we found a compound having the same composition and similar cell parameters. However, the crystallographic information file (CIF) is only found for a neodymium single-crystal analogue.

In fact, the hexaborate chain in compounds 1 and 2 (Figure 4a) has also been observed in other borate compounds, such as  $(\text{Li}_{5.5}\text{Fe}_{0.5})\text{FePb}(\text{B}_6\text{O}_{12})_2$ <sup>15</sup> and  $\text{NaNdB}_6\text{O}_9(\text{OH})_4$ <sup>4</sup> (Figure 4b). In the structure of  $(\text{Li}_{5.5}\text{Fe}_{0.5})\text{FePb}(\text{B}_6\text{O}_{12})_2$ , the hexaborate

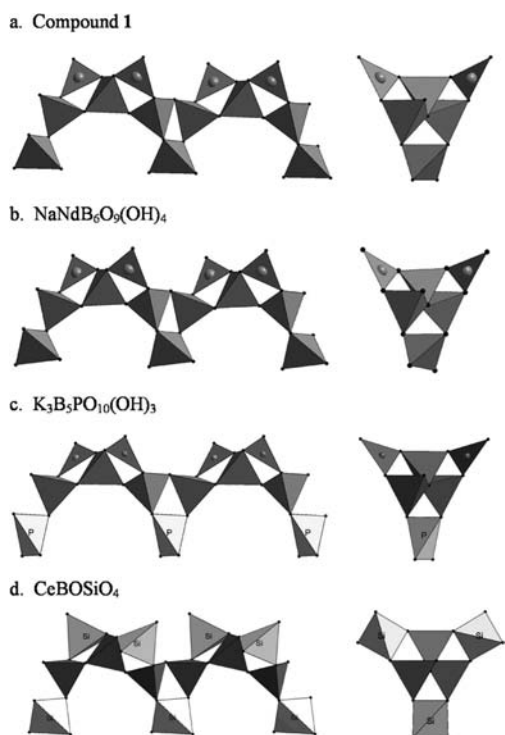


**Figure 4.** Similar chains in compounds **1** (a),  $\text{NaNdB}_6\text{O}_9(\text{OH})_4$  (b),  $\text{K}_3\text{B}_5\text{PO}_{10}(\text{OH})_3$  (c), and  $\text{CeBOSiO}_4$  (d). The images in the right side are a view from perpendicular to the chains.

chain is formed with  $3\text{T} + 3\Delta$ , whereas in the structure of  $\text{NaNdB}_6\text{O}_9(\text{OH})_4$ , the chain is formed with  $4\text{T} + 2\Delta$ , the same as in compounds **1** and **2**. This type of chain also occurs in mixed borates. In the structure of  $\text{K}_3\text{B}_5\text{PO}_{10}(\text{OH})_3$ ,<sup>16</sup> one  $\text{BO}_4$  tetrahedron in the borate chain is replaced by a  $\text{PO}_4$  tetrahedron (Figure 4c), whereas in the structure of stillwellite  $\text{CeBOSiO}_4$ ,<sup>17</sup> one  $\text{BO}_4$  tetrahedron and both  $\text{BO}_3$  trigonal units are replaced by  $\text{SiO}_4$  tetrahedra, forming a chain with only tetrahedra (Figure 4d). The condensed structures have been assured by Li, Fe, and Pb in  $(\text{Li}_{5.5}\text{Fe}_{0.5})\text{FePb}(\text{B}_6\text{O}_{12})_2$  and Na and Nd in  $\text{NaNdB}_6\text{O}_9(\text{OH})_4$ , respectively. However, in compounds **1** and **2**, hexaborate chains are connected by  $\text{SmO}_8$  polyhedra, forming a condensed layer. Interactions between neighboring layers are assured by hydrogen bonds involving the oxygen atoms in the condensed 2D layer and OH groups of isolated boric acid molecules  $\text{B}(\text{OH})_3$ . Further structural analysis indicates that the 2D layers of compounds **1** and **2** are very similar to that of  $\text{NaNdB}_6\text{O}_9(\text{OH})_4$ . In the  $\text{NdB}_6\text{O}_9(\text{OH})_4$  layer,  $\text{Nd}^{3+}$  is coordinated to nine oxygen atoms with one Nd–O bond distance at 2.818(3) Å. This oxygen atom also coordinates to neighboring  $\text{Nd}^{3+}$ . The two  $\text{NdO}_9$  polyhedra form a dimer by coordinating this oxygen from each polyhedron to a neighboring one, with a metal–metal distance of 4.333 Å. Without considering this oxygen, the coordination geometry of  $\text{NdO}_8$  is very similar to those samarium polyhedra in compounds **1** and **2**. This is not surprising because ionic radii of  $\text{Nd}^{3+}$  (1.109 Å) and  $\text{Sm}^{3+}$  (1.079 Å) in 8-coordination are very similar. In compounds **1** and **2**, the nearest oxygen atoms from neighboring polyhedra are 2.986 (**1**) and 3.083 (**2**) Å, and the metal–metal distance is 4.436 (**1**) and 4.514 (**2**) Å, respectively. The  $\text{NaNdB}_6\text{O}_9(\text{OH})_4$  material has been prepared hydrothermally at 270–280 °C for 18–20 days under a pressure of about 70 atm. Figure 5 represents the structures of

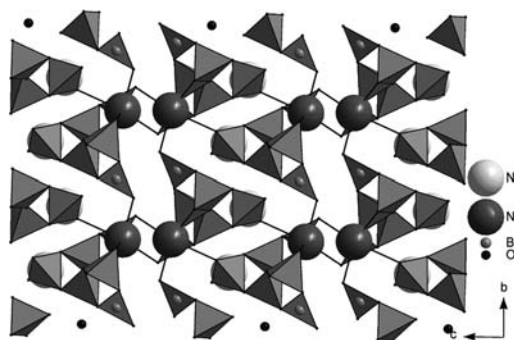


**Figure 5.** Structural representation of  $\text{NaNdB}_6\text{O}_9(\text{OH})_4$ .

$\text{NaNdB}_6\text{O}_9(\text{OH})_4$  viewed along the  $a$  direction. Clearly, the difference between  $\text{NaNdB}_6\text{O}_9(\text{OH})_4$  and compounds **1** and **2** lies on the connectivity of the layers. In the structures of  $\text{NaNdB}_6\text{O}_9(\text{OH})_4$ , sodium coordinates to the oxygen atoms from neighboring 2D layers, forming a dense structure. In fact, both compound **1** and  $\text{NaNdB}_6\text{O}_9(\text{OH})_4$  crystallize in the same space group (PT) with similar  $a$  and  $b$  axes and a different  $c$  axis due to the existence of boric acid between the layers in compound **1** ( $a = 6.799$  Å,  $b = 7.167$  Å,  $c = 10.297$  Å,  $\alpha = 86.37^\circ$ ,  $\beta = 103.85^\circ$ ,  $\gamma = 102.24^\circ$  for  $\text{NaNdB}_6\text{O}_9(\text{OH})_4$ ). Therefore, compounds **1** and **2** and  $\text{NaNdB}_6\text{O}_9(\text{OH})_4$ , although they have different compositions, can be considered as the same family. Belokoneva also pointed out that the polar arrangement of such a chain in the structures may give ferroelectric crystals as stillwellite derivatives ( $\text{LaBGeO}_5$ ,  $\text{PrBGeO}_5$ ).<sup>18</sup> The isolated  $\text{BO}_3$  triangle also occurs in other polyborate materials, such as the minerals gowertite  $[\text{CaB}_5\text{O}_8(\text{OH}) \cdot \text{B}(\text{OH})_3 \cdot 3\text{H}_2\text{O}]$ <sup>19</sup> and veatchite  $[\text{Sr}_2[\text{B}_5\text{O}_8(\text{OH})]_2 \cdot \text{B}(\text{OH})_3 \cdot \text{H}_2\text{O}]$ <sup>20</sup> and synthetic  $\text{Ca}_2[\text{B}_5\text{O}_8(\text{OH})]_2 \cdot \text{B}(\text{OH})_3 \cdot \text{H}_2\text{O}$ ,<sup>21</sup> and interacts with the structural framework by hydrogen bonds.  $\text{Ca}_2[\text{B}_5\text{O}_8(\text{OH})]_2 \cdot \text{B}(\text{OH})_3 \cdot \text{H}_2\text{O}$  was prepared hydrothermally at 280 °C for 20 days in 15% chloride–carbonate solutions at a  $\text{B}_2\text{O}_3/\text{CaO}$  weight ratio of 2.5 and a pH between 5 and 6.<sup>21</sup>

The thermal stability of compound **3** is higher than that of compound **2**. The decomposition of compound **3** starts at ca. 510 °C, whereas that of compound **2** starts at ca. 330 °C. The structure loses water before it is fully decomposed. From structure data, the hydrogen bonding of water in compound **3** is weaker than that in compound **2**. However, it loses water at a relative high temperature, which may be due to the small window of the framework structure. To study the stability of compound **3** after dehydration, the crystals have been calcined at 415 °C for 90 min and studied by single-crystal X-ray analysis. The dehydrated compound **3** showed cell expansion along the  $a$  and  $b$  axes, and shrinkage in the  $c$  axis after dehydration, and the total cell volume is slightly big after dehydration ( $a = 8.1538(2)$  Å,  $b = 16.6788(5)$  Å,  $c = 9.8053(3)$  Å,  $V = 1333.48(7)$  Å<sup>3</sup>). Unfortunately, the dehydrated compound **3** is not suitable for single-crystal XRD structure determination. Considering the structure similarity of compounds **1** and **2**, compound **2** was dehydrated at 290 °C for 1 h. However, it does not transform to compound **1**. The distance between dense layers decreases, giving clear XRPD diffraction peaks at  $d$ -spacings of 11.28, 5.65, and 3.78 Å. We suspect that  $\text{H}_3\text{BO}_3$  between the layers may be dehydrated as the structure water was removed since the first step mass loss is higher than that of the theoretic one for one water removal (3.54 wt %).  $\text{H}_3\text{BO}_3$  dehydrates above 170 °C, forming metaboric acid

(HBO<sub>2</sub>). Metaboric acid melts at ca. 236 °C and further dehydrates above ca. 300 °C, forming tetraboric acid (H<sub>2</sub>B<sub>4</sub>O<sub>7</sub>). With this consideration, compound **2** was treated at low temperature. The structure of compound **2** maintains after being treated at 80 °C for 3 days. After being treated at 130 °C for 2 days, a peak at a *d*-spacing of 12.39 Å significantly increased in the XRPD pattern, which is just at the same position of the first diffraction peak of compound **1**. Unfortunately, after treatment, the sample is not suitable for single-crystal XRD studies. Furthermore, since the dense layer of compound **2** is similar to that of NaNdB<sub>6</sub>O<sub>9</sub>(OH)<sub>4</sub>, compound **2** was treated with diluted NaOH solution. A 100 mg portion of compound **2** was added into 10 mL of NaOH solution (with a Na/Sm ratio of 6) and kept at room temperature for 3 days without agitation. The solid was separated from the solution by filtration with filter paper, washed with distilled water, and dried at room temperature. The run product shows slight decreases of the distance between dense layers, giving clear XRPD diffraction peaks at *d*-spacings of 13.23 and 6.64 Å. The compound **2** was then treated with 0.76 M NaCl solution. A 76 mg portion of compound **2** was added into 10 mL of NaCl solution and kept at room temperature for 3 days without agitation. The XRPD pattern of this sample displayed a new intensive peak at a *d*-spacing of 10.11 Å and a new hump around a *d*-spacing of 5.04 Å. NaNdB<sub>6</sub>O<sub>9</sub>(OH)<sub>4</sub> gives the first diffraction peak at a *d*-spacing of 9.997 Å. Both experiments suggest that, after treatment, the materials still maintained layered characteristics. Finally, considering that the annealing of rare earth polyborates at moderate temperature may produce metastable anhydrous pentaborates,<sup>1,2</sup> compound **2** was heated at high temperature. The sample after heat treatment at 650 °C for 5 days maintains its habit only with some cracks. However, the XRD indicates its amorphous characteristic without any diffraction peaks. The sample after heat treatment at 750 °C for 2 days transformed to an unknown crystalline phase, a different phase to that reported in the literature.<sup>1,2</sup> XRPD patterns of compound **2** after different treatments are shown in Figure S4 (Supporting Information).

## CONCLUSIONS

We have demonstrated that the synthesis of samarium polyborate is very sensitive to the experimental conditions. With slight modification of synthesis conditions, three samarium polyborates have been crystallized. The two layered materials are structurally related and constituted by hexaborate chains. SmB<sub>9</sub>O<sub>13</sub>(OH)<sub>4</sub>·H<sub>2</sub>O can be obtained with or without adding water to the reaction. The possible relationship between new phases and existing phases has been discussed. The preliminary tests indicated that the new layered samarium borate compound **2** may be able to transform to compound **1** and NaNdB<sub>6</sub>O<sub>9</sub>(OH)<sub>4</sub> by careful selection of treatment conditions. The sensitivity of the studied system to variations in the reaction temperature and precursor reagents is indicative that the preparation of lanthanide borate compounds with tailored structures depends on the appropriate choice of physicochemical conditions.

## ASSOCIATED CONTENT

### Supporting Information

SEM images, crystallographic information files, bond lengths and bond angles, polyhedral representation of SmO<sub>8</sub> and SmO<sub>9</sub>, and borate clusters. This material is available free of

charge via the Internet at <http://pubs.acs.org>. Crystallographic data for compounds **1–3** have been deposited to the FIZ Karlsruhe Crystallographic Data Center allocated with the deposit number CSD 423821-423823.

## AUTHOR INFORMATION

### Corresponding Author

\*E-mail: [zlin@ua.pt](mailto:zlin@ua.pt).

### Present Address

<sup>†</sup>The School of Chemistry and Biological Engineering, Suzhou University of Science and Technology, 1 Kerui Road, Suzhou 215009, Jiangsu, China.

### Notes

The authors declare no competing financial interest.

## ACKNOWLEDGMENTS

This work was supported by FCT, POCI2010, PTDC/CTM/73643/2006, FSE, and FEDER.

## REFERENCES

- (1) Li, L. Y.; Lu, P. C.; Wang, Y. Y.; Jin, X. L.; Li, G. B.; Wang, Y. X.; You, L. P.; Lin, J. H. *Chem. Mater.* **2002**, *14*, 4963–4968.
- (2) Li, L. Y.; Jin, X. L.; Li, G. B.; Wang, Y. X.; Liao, F. H.; Yao, G. Q.; Lin, J. H. *Chem. Mater.* **2003**, *15*, 2253–2260.
- (3) Cong, R. H.; Yang, T.; Wang, Z. M.; Sun, J. L.; Liao, F. H.; Wang, Y. X.; Lin, J. H. *Inorg. Chem.* **2011**, *50*, 1767–1774.
- (4) Belokoneva, E. L.; Ivanova, A. G.; Dimitrova, O. V. *Russ. J. Inorg. Chem.* **2006**, *51*, 869–877.
- (5) Belokoneva, E. L.; Shagivaleeva, I. K.; Dimitrova, O. V.; Mochonova, N. N. *Crystallogr. Rep.* **2010**, *55*, 753–759.
- (6) Belokoneva, E. L.; Stefanovich, S. Y.; Dimitrova, O. V.; Ivanova, A. G. *Russ. J. Inorg. Chem.* **2002**, *47*, 317–323.
- (7) Sun, H. Y.; Zhou, Y.; Huang, Y. X.; Sun, W.; Mi, J. X. *Chin. J. Struct. Chem.* **2010**, *29*, 1387–1393.
- (8) Li, L. Y.; Liao, F. H.; Li, G. B.; Lin, J. H. *Chin. J. Inorg. Chem.* **2005**, *21*, 949–954.
- (9) Ivanova, A. G.; Belokoneva, E. L.; Dimitrova, O. V.; Mochonova, N. N. *Crystallogr. Rep.* **2006**, *51*, 584–588.
- (10) Ivanova, A. G.; Belokoneva, E. L.; Dimitrova, O. V.; Mochonova, N. N. *Russ. J. Inorg. Chem.* **2006**, *51*, 862–868.
- (11) Ivanova, A. G.; Belokoneva, E. L.; Dimitrova, O. V. *Russ. J. Inorg. Chem.* **2004**, *49*, 816–822.
- (12) Abdylayev, G. K.; Dzhabarov, G. G.; Mamedov, K. S. *Kristallografiya* **1984**, *29*, 1084–1088.
- (13) Belokoneva, E. L. *Cryst. Rev.* **2005**, *11*, 151–198.
- (14) Sheldrick, M. *Shelx-97: Program for the Solution of Crystal Structures*; University of Göttingen: Göttingen, Germany, 1997.
- (15) Belokoneva, E. L.; Ruchkina, E. A.; Dimitrova, O. V. *Russ. J. Inorg. Chem.* **2001**, *46*, 20–27.
- (16) Hauf, C.; Kniep, R. Z. *Kristallogr.* **1996**, *211*, 707–708.
- (17) Voronkov, A. A.; Pyatenko, Yu. A. *Kristallografiya* **1967**, *12*, 258–265.
- (18) Belokoneva, E. L. *Cryst. Res. Technol.* **2008**, *43*, 1173–1182.
- (19) Konner, J. A.; Clark, J. R.; Christ, C. L. *Am. Mineral.* **1972**, *57*, 381–396.
- (20) Clark, J. R.; Christ, C. L. *Am. Mineral.* **1971**, *56*, 1934–1954.
- (21) Yamnova, N. A.; Zubkova, N. V.; Dimitrova, O. V.; Mochonova, N. N. *Crystallogr. Rep.* **2009**, *54*, 800–813.